Published OnlineFirst June 4, 2008; DOI: 10.1158/1535-7163.MCT-08-0104

Human rhomboid family-1 gene silencing causes apoptosis or autophagy to epithelial cancer cells and inhibits xenograft tumor growth

Zhenwen Yan,[1] Huafei Zou,[1] Fang Tian,[1] Jennifer R. Grandis,[2] A. James Mixson,[3] Patrick Y. Lu,[4] and Lu-Yuan Li[1]

Departments of [1]Pathology and [2]Otolaryngology, University of Pittsburgh School of Medicine, Pittsburgh, Pennsylvania; [3]Department of Pathology, University of Maryland School of Medicine, College Park, Maryland; and [4]Sirnaomics, Inc., Rockville, Maryland

Abstract

The rhomboid family of genes carry out a wide range of important functions in a variety of organisms. Little is known, however, about the function of the human rhomboid family-1 gene (RHBDF1). We show here that RHBDF1 function is essential to epithelial cancer cell growth. RHBDF1 mRNA level is significantly elevated in clinical specimens of invasive ductal carcinoma of the breast, and the protein is readily detectable in human breast cancer or head and neck cancer cell lines. Silencing the RHBDF1 gene with short interfering RNA (siRNA) results in apoptosis in breast cancer MDA-MB-435 cells and autophagy in head and neck squamous cell cancer 1483 cells. The treatment also leads to significant down-modulation of activated AKT and extracellular signal-regulated kinase in the cells, suggesting that critically diminished strength of these growth signals may be the key attributes of the induction of cell death. Furthermore, silencing the RHBDF1 gene in MDA-MB-435 or 1483 xenograft tumors on athymic nude mice by using i.v. administered histidine-lysine polymer nanoparticle-encapsulated siRNA results in marked inhibition of tumor growth. Our findings indicate that RHBDF1 has a pivotal role in sustaining growth signals in epithelial cancer cells and thus may serve as a therapeutic target for treating epithelial cancers. [Mol Cancer Ther 2008;7(6):1355–64]

Received 1/28/08; revised 3/27/08; accepted 3/30/08.

Grant support: Flight Attendant Medical Research Institute and Henry L. Hillman Foundation (L-Y. Li) and National Cancer Institute Head and Neck SPORE CA097190 (J.R. Grandis).

The costs of publication of this article were defrayed in part by the payment of page charges. This article must therefore be hereby marked *advertisement* in accordance with 18 U.S.C. Section 1734 solely to indicate this fact.

Note: Current address for Z. Yan: Department of Neurology, Sun Yat-Sen University, Guangdong, People's Republic of China.

Requests for reprints: Lu-Yuan Li, University of Pittsburgh Cancer Institute, 5117 Centre Avenue, G12C, Pittsburgh, PA 15213. Phone: 412-623-1118; Fax: 412-623-4747. E-mail: lil@upmc.edu

doi:10.1158/1535-7163.MCT-08-0104

Introduction

The rhomboid family of genes encode a group of proteins with six- or seven-transmembrane domains found in wide range of organisms (1). The prototype rhomboid gene was first discovered in *Drosophila*, where it is a critical component of epidermal growth factor receptor signaling pathway during development (2). The functions of known rhomboid proteins, despite similarity in tertiary structures, are highly diverse, including quorum sensing in bacteria (3), mitochondrial membrane fusion (4), differentiation and maintenance of neural progenitors (5), and stem cell differentiation in eukaryotes (6). Modulation of cell signaling is apparently the main function of rhomboid proteins, although their mechanisms of function in human remain largely unknown. The human rhomboid family-1 gene RHBDF1 (accession no. NM_022450) is a seven-transmembrane protein. Like its homologue in the fruit fly, it is located on the endoplasmic reticulum and Golgi (7). Unlike the *Drosophila* protein, there is no experimental evidence to indicate that RHBDF1 activates epidermal growth factor–like growth factors through proteolytic cleavage of the ligand precursors, despite the finding that the RHBDF1 protein may interact with transforming growth factor-α, a ligand of epidermal growth factor receptor (7).

We present experimental evidence here to support our hypothesis that the RHBDF1 gene is a potential target for the development of therapeutic approaches to treat breast and head and neck cancers and possibly other epithelial cell cancers. We show that RHBDF1 gene expression is significantly elevated in clinical specimens of early-stage breast cancer. We used two different cancer models, namely, human breast cancer cell line MDA-MB-435 and human head and neck squamous cell cancer cell line 1483 and their respective xenograft tumors, to show that silencing the gene with short interfering RNA (siRNA) causes apoptosis and autophagy of the cancer cells and inhibition of xenograft tumor growth. In addition, we show that delivery of siRNA to established xenograft tumors can be achieved by using i.v. administered histidine-lysine polymer (HKP)–encapsulated siRNA. Our data suggest that RHBDF1 is critically involved in the modulation of growth signals essential to epithelial cancers.

Materials and Methods

Materials

Human breast cancer cell lines were purchased from the American Type Culture Collection. Human head and neck squamous cell carcinoma cell lines were as described (8). Rabbit polyclonal antibody against RHBDF1 was generated with a synthetic RHBDF1 peptide MSEARRDSTS SLQRKKPC, purified by affinity chromatography, and

Published OnlineFirst June 4, 2008; DOI: 10.1158/1535-7163.MCT-08-0104

verified by the loss of the ability of antibody to detect the target protein in Western blotting analysis in the presence of the peptide.

Determination of Gene Expression Profiles in Human Cancer Specimens

The ASCENTA System from Gene Logic was used. Human clinical specimens were collected and verified by the vendor's board-certified pathologists and according to institutional review board–approved protocols. Total RNA was analyzed by using the Affymetrix Human Genome U133 GeneChip array and Affymetrix Microarray Suite (version 5.0) and LIMS (version 3.0). The expressed sequence tag and serial analysis of gene expression data in the National Cancer Institute Cancer Genome Anatomy Project databases were used.[5] The Kruskal-Wallis test and Wilcoxon test were used to determine differences between groups.

RHBDF1 siRNA Molecules

Eight of 19-mer sequences against RHBDF1 cDNA sequence were designed using public domain algorithms. Three of these siRNA molecules, RH1-1, RH1-2, and RH1-3, corresponding to coding sequences starting at positions 173, 210, and 379, respectively, were selected: RH1-1 (forward) 5′-AGCUGGACAUUCCCUCUGCdTdT-3′ and (reverse) 5′-GCAGAGGGAAUGUCCAGCUdTdT-3′, RH1-2 (forward) 5′-GAGCCCAGCUUCCUGCAGCdTdT-3′ and (reverse) 5′-GCUGCAGGAAGCUGGGCUCdTdT-3′, and RH1-3 (forward) 5′-GAGUGAGCAAGGACAGUGAdTdT-3′ and (reverse) 5′-UCACUGUCCUUGCUCACUCdTdT-3′. Two siRNA molecules that exhibit no homology to human genome sequence were selected as negative controls: CT-1 (forward) 5′-CAGUUGCGCAGCCUGAAUGdTdT-3′ and (reverse) 5′-CAUUCAGGCUGCGCAACUGdTdT-3′ and 3′-Alexa Fluor 555–labeled CT-2 (forward) 5′-GCUGACC-CUGAAGUUCAUCUGCAdTdT-3′ and (reverse) 5′-UGCAGAUGAACUUCAGGGUCAGCdTdT-3′.

RHBDF1 Gene Silencing *In vitro*

Cells were transfected using a HiperFect transfection protocol (Qiagen). Briefly, the cells were seeded (2×10^4 per well) in a 12-well plate in 0.5 mL DMEM. The siRNA was diluted in 0.1 mL serum-free Opti-MEM, mixed with 3 μL of the transfection reagent, incubated for 10 min at room temperature, and then added drop-wise into the cell culture. Target mRNA and protein levels and effects on cells were analyzed in 48 h.

Analysis of Apoptosis

Coverslips containing harvested cells were fixed with 4% paraformaldehyde, incubated in 0.1% Triton X-100 then with terminal deoxynucleotidyl transferase–mediated dUTP nick end labeling reaction mixture (Roche Molecular Biochemicals) containing FITC-conjugated dUTP, and Hoechst (100 ng/mL), and then sealed for fluorescent microscopic analysis. The ratio of the number of apoptotic cells (green fluorescent) to total number of cells (blue fluorescent nuclei) was determined using image analysis software Image-J (NIH). At least 1,000 cells on each coverslip were analyzed.

[5] http://cgap.nci.nih.gov/

Analysis of Autophagy

Cell autophagy was determined as described (9). Briefly, cells were seeded in 12-well plates with coverslips (1,500 per well) and transfected with 2 μg/mL siRNA. After 24-h incubation at 37°C, 5% CO_2, cells were transfected with green fluorescent protein-light chain 3 (LC3) and cultured in DMEM for 48 h, fixed with 4% paraformaldehyde, and incubated in 0.1% Triton X-100. Blocked with 5% bovine serum albumin for 1 h, the cells were incubated with a green fluorescent protein antibody (Santa Cruz Biotechnology) for 1 h and then with an Alexa Fluor 488–conjugated secondary antibody (Invitrogen) together with Texas red–conjugated phalloidin for 1 h at room temperature. Further incubated with Hoechst for 5 min, the coverslips were sealed and subjected to fluorescent microscopic analysis. At least 300 cells on each coverslip were counted. The lipidation of LC3, which marks the onset of autophagy, is also determined by Western blotting as described (10).

Analysis of Cell Proliferation

Coverslips containing harvested cells were fixed with 4% paraformaldehyde, incubated in 0.1% Triton X-100, and blocked with 5% bovine serum albumin for 1 h and then incubated with a polyclonal antibody ab833 (Abcam) against proliferating cell nuclear marker Ki-67 then with Texas red–labeled anti-rabbit antibody (Vector Laboratories) then with Hoechst (100 ng/mL) for 5 min, sealed, and subjected to fluorescent microscopic analysis. The ratio of proliferating cells (red) to total number of cells (blue) was determined by using Image-J. At least 1,000 cells on each coverslip were analyzed.

ELISA Assay

The MDA-MB-435 or 1483 cells were seeded in 96-well plates (1.4×10^4 per well), treated for 10 min with either the control siRNA or the RHBDF1 siRNA (2 μg/mL) mixed with Hi-Perfect transfection reagent, and incubated overnight at 37°C, 5% CO_2. The culture media were changed with fresh ones but without fetal bovine serum and continued incubation for 48 h. Extracellular signal-regulated kinase (ERK) 1/2 phosphorylation was then measured by using an ELISA assay (SuperArray Bioscience), which uses specific primary antibodies against either phospho-ERK1/2 or total ERK1/2 and horseradish peroxidase–conjugated secondary antibodies according to the manufacturer's instructions.

Reverse Transcription-PCR

Total RNA was extracted from cell culture or tumor tissue with RNeasy mini kit (Qiagen) according to the manufacturer's instructions. For reverse transcription (RT-PCR), the first cDNA strands were synthesized by using cDNA Synthesis Kit (GE Healthcare) according to the manufacturer's instructions. Primers for RHBDF1 are sense 5′-GGGCTGCTGCCGTGGATTGA-3′ and antisense 5′-GGCTCAGGGAGGTCGTGTCT-3′. Primers for glyceraldehyde-3-phosphate dehydrogenase are sense 5′-GTCAACG-GATTTGGTCTGTATT-3 and antisense 5-AGTCTT-CTGGGTGGCAGTGAT-3′. The thermal cycle profile was as follows: denaturing for 1 min at 94°C, annealing for 1 min at 59°C, and extension for 1 min at 72°C.

Published OnlineFirst June 4, 2008; DOI: 10.1158/1535-7163.MCT-08-0104

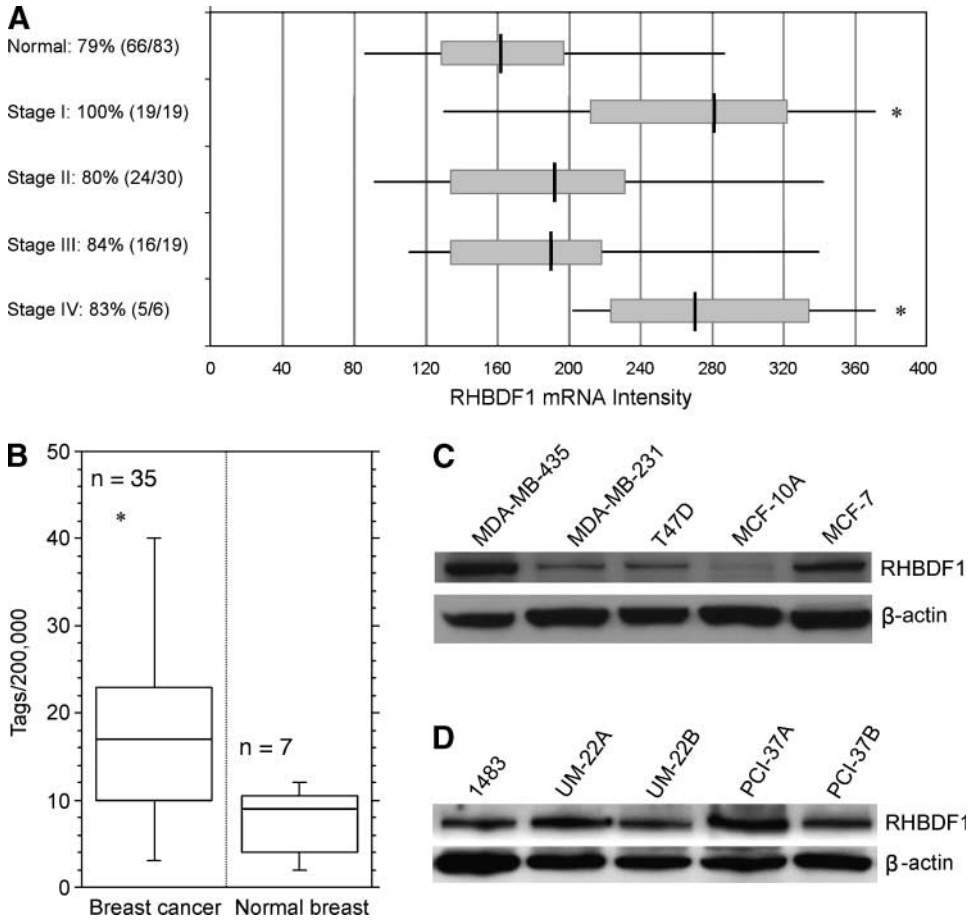

Figure 1. RHBDF1 expression profile in epithelial cancer clinical specimens and cell lines. **A,** box plot of microarray analysis of RHBDF1 mRNA levels in breast cancer specimens at four stages of IDC and normal breast tissues. *Boxes,* data ranges from the 25th percentile to the 75th percentile; *vertical bars,* median; *horizontal lines,* minimum and maximum. *, $P < 0.01$ comparing median of the tumors with that of the normal tissues (Newman-Keuls' methods). **B,** box plot of the number of established sequence tags as a measure of RHBDF1 mRNA abundance in breast cancer specimens and normal breast tissues. *Horizontal bars,* median. *, $P < 0.02$, ANOVA. **C,** Western blotting analysis of the RHBDF1 protein in breast cancer cell lines MDA-MB-435, MDA-MB-231, T47D, and MCF-7 and a nontumorigenic breast epithelial cell line MCF-10A. **D,** Western blotting analysis of the RHBDF1 protein in head and neck squamous cancer cell lines 1483, UM-22A, UM-22B, PCI-37A, and PCI-37B.

Delivery of siRNA Using poly-HKP

The branched histidine (H) and lysine (K) polymers used in this study were R-KR-KR-KR, where *R* = [HHHKHHHKHHHKHHH]2KH4NH4, and H3K4b, a branched polymer with the same core and structure, except that the R branches differ: *R* = KHHHKHHHKHH-HKHHHK, basically as described (11). The HKP was dissolved in aqueous solution and then mixed with a siRNA aqueous solution at a ratio of 4:1 by mass, forming nanoparticles with an average size of 150 to 200 nm in diameter. The HKP-siRNA solutions can be stored at 4°C for at least 3 months.

Fluorescence-Conjugated siRNA Distribution in Mouse Tissues and Xenograft Tumors

Female athymic nude mice bearing 1483 xenograft tumors (average volume, 100 mm^3) received tail vein injection of HKP-encapsulated, fluorescence-conjugated siRNA CT-2. The animals were sacrificed at 1 or 60 min. The organs and tumor were retrieved and freshly frozen in Tissue Freezing Medium (Sakura Finetek), sectioned (5 μm), or immunostained for PECAM (CD31; BD Biosciences) and subjected to fluorescent microscopic analysis (Nikon Eclipse E800).

Human Cancer Xenograft Tumor Models

Six- to 8-week-old female athymic nude mice (Taconic Farms) were used. Human breast cancer MDA-MB-435 cells (4×10^5) in 50 μL serum-free DMEM were injected into the mammary fat pads. Human head and neck squamous cell cancer 1483 cells (1×10^6) in 50 μL Matrigel (30%) were s.c. injected on the flanks. When the tumors became palpable (~50 mm^3), the animals were randomized, regrouped, and treated with tail vein injections of HKP-siRNA solutions (40 μg siRNA in 50 μL of HKP) at 4- or 5-day intervals in a blinded manner. Tumor volumes were determined by measuring the lengths and widths of the tumors using the equation: $V = 0.52 \times \text{length} \times \text{width} \times \text{width}$. The care and use of all experimental animals were according to the University of Pittsburgh Institutional Animal Care and Use Committee approved protocols.

Statistics

All cell culture experiments were carried out in triplicate and repeated at least two times. Animal experiments had five to eight animals per group as indicated, and the experiments was each repeated once. Data are presented as mean ± SD. Statistic analysis methods used are indicated in the text. $P < 0.05$ was considered significant.

Published OnlineFirst June 4, 2008; DOI: 10.1158/1535-7163.MCT-08-0104

Results

RHBDF1 Expression Is Elevated in Breast Cancer Clinical Specimens

We determined RHBDF1 gene expression levels in human normal breast tissues and clinical specimens of all four stages of invasive ductal carcinoma (IDC; Fig. 1A). We found that the RHBDF1 transcript was readily detectable in all (100% or 19 of 19) IDC stage I tumors, whereas the percentages of RHBDF1-positive samples in IDC stages II to IV were similar to that in the normal breast, which was 79% (66 of 83). More interestingly, the relative intensity of RHBDF1 mRNA in IDC stage I samples was nearly two times higher than the normal value. In addition, whereas RHBDF1 mRNA levels in IDC stages II and III showed only marginal increases compared with the normal values, there was once again a statistically significant increase in stage IV samples, with a median value reaching that of the stage I samples. To corroborate this finding, we carried out data mining of the National Cancer Institute Cancer Genome Anatomy Project databases. We found that the abundance of RHBDF1 expressed sequence tags in breast cancer specimens was ~2-fold that in normal breast (Fig. 1B). These data suggest that RHBDF1 gene may be functional in normal epithelial cells in the breast and that its expression is significantly up-regulated during the development of breast cancer.

RHBDF1 Is Present in Epithelial Cancer Cell Lines

We determined RHBDF1 gene expression at protein level in four human breast cancer cell lines, including MDA-MB-435, MDA-MB-231, T47D, and MCF-7. The RHBDF1 protein was readily detectable in all these cell lines at different levels when the total cell lysates were analyzed (Fig. 1C). We also determined RHBDF1 protein level in a spontaneously immortalized, nontumorigenic breast epithelial cell line MCF-10A and found that the RHBDF1 protein was at a substantially lower level in this cell line than in other cell lines. In addition, we determined RHBDF1 protein levels in five head and neck cancer cell lines derived from primary tumors and metastases for comparison, including 1483, UM-22A, UM-22B, PCI-37A, and PCI-37B cells. These data indicate that RHBDF1 protein is produced in breast cancer and head and neck cancer cells.

RHBDF1 Gene Silencing in MDA-MB-435 Breast Cancer Cells Leads to Growth Inhibition and Apoptosis

To determine the RHBDF1 gene function, we silenced this gene by transfecting the human breast cancer MDA-MB-435 cells with siRNA molecules targeting RHBDF1 mRNA and then analyzed the effect on cell growth and survival. Effective elimination of RHBDF1 mRNA in MDA-MB-435 cells was achieved, as determined by RT-PCR analysis of total RNA preparations of these cells (Fig. 2A), by using siRNA molecules RH1-1, RH1-2, and RH1-3, which respectively targeted nucleotide position numbers 173, 210, or 379 of the RHBDF1 mRNA open reading frame. Cells in the control groups were treated with a siRNA, CT-1, which had a randomized nucleotide sequence that had no significant homology to any part of the human genome. The effectiveness of these siRNA molecules was confirmed by examining the RHBDF1 protein levels by Western blotting (Fig. 2A).

Silencing the RHBDF1 gene in MDA-MB-435 cells led to a significant inhibition of cancer cell proliferation. The percentage of proliferating cells (Ki-67 positive) decreased from ~85% in the control cells to ~20% to 30% in the experimental groups (Fig. 2B). The growth inhibition resulted from apoptotic cell death. Each of the three

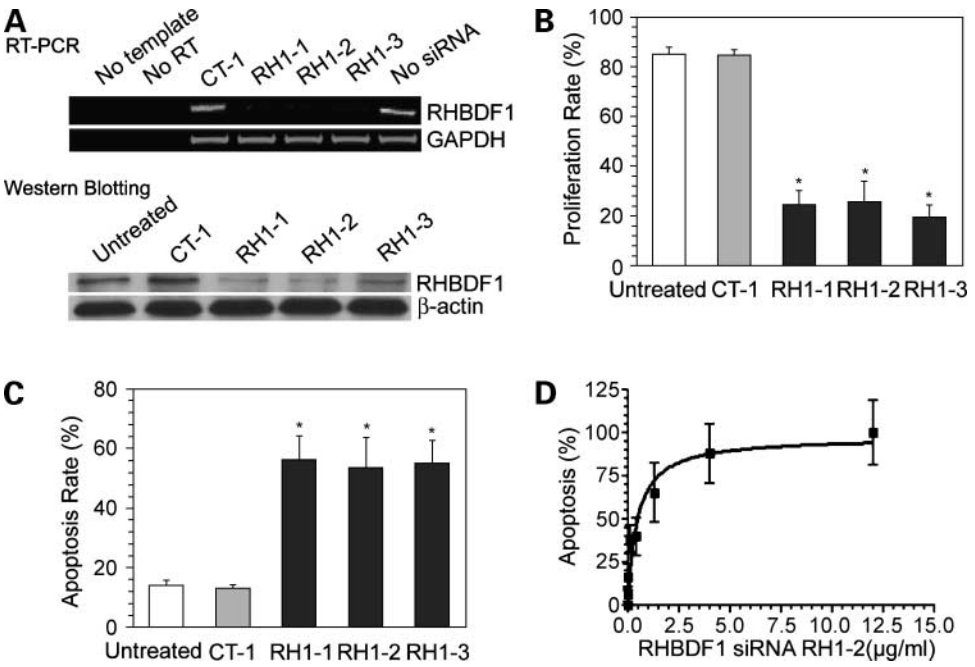

Figure 2. RHBDF1 gene silencing in MDA-MB-435 breast cancer cells causes growth inhibition and apoptosis. **A,** RT-PCR and Western blotting analyses of RHBDF1 mRNA levels following treatment with RHBDF1 siRNA molecules RH1-1, RH1-2, RH1-3, or a control siRNA CT-1 (10 μg/mL each). Other controls include the absence of RNA sample (*No Template*), reverse transcriptase (*No RT*), or exogenous siRNA (*No siRNA*) in the reaction mixtures. **B,** percentage of proliferating cells (Ki-67 positive) following treatment with the indicated siRNA molecules (2 μg/mL). **C,** percentage of apoptotic cells following treatment with either the control siRNA or the RHBDF1 siRNA molecules (2 μg/mL). **D,** dose-dependent induction of apoptosis by RH1-2 treatment. Mean ± SD of triplicate experiments. *, $P < 0.05$, ANOVA.

Published OnlineFirst June 4, 2008; DOI: 10.1158/1535-7163.MCT-08-0104

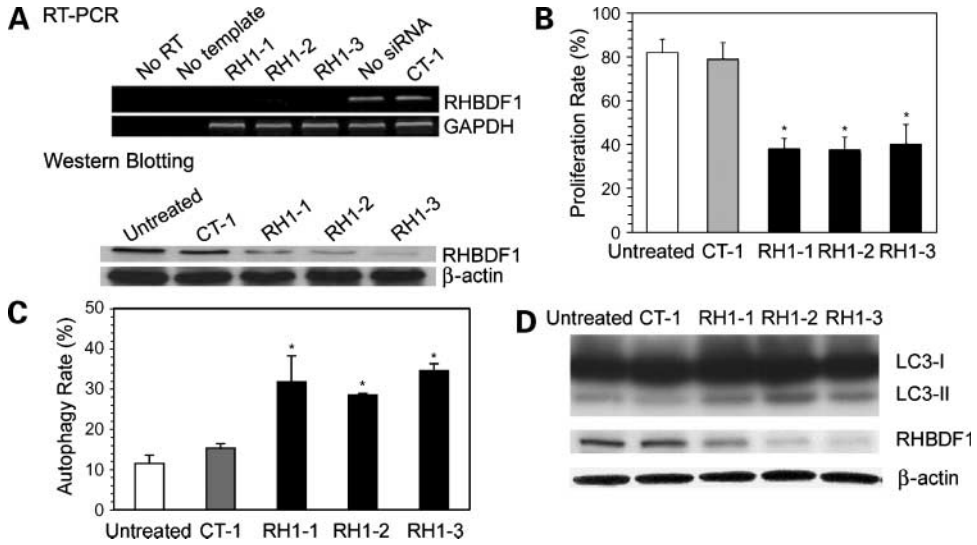

Figure 3. RHBDF1 gene silencing in head and neck squamous cancer 1483 cells causes growth inhibition and autophagy. **A,** RT-PCR and Western blotting analyses of RHBDF1 mRNA levels following treatment with RHBDF1 siRNA molecules RH1-1, RH1-2, RH1-3, or a control siRNA CT-1 (10 μg/mL). Other controls include the absence of the reverse transcriptase, the RNA sample, or exogenous siRNA in the reaction mixtures. **B,** percentage of proliferating cells (Ki-67 positive) following treatment with each of the indicated siRNA molecules (2 μg/mL). **C,** percentage of cells containing autophagosomes. Mean ± SD of duplicated cultures. **D,** Western blotting analysis of LC3I and the autophagy marker LC3II. Increased amount of LC3II in RHBDF1 siRNA treatment groups. RHBDF1 expression levels were simultaneously determined. *, $P < 0.05$, ANOVA.

RHBDF1 siRNA molecules at a final concentration of 10 μg/mL was effective in apoptosis induction in MDA-MB-435 cells, causing an increase of the number of apoptotic cells from ~10% in the control groups to ~60% in the experimental groups (Fig. 2C). The induction of apoptosis in MDA-MB-435 cells by the siRNA treatment was dose dependent, yielding a half-maximum inhibition concentration (IC_{50}) of ~1 μg/mL (Fig. 2D). These results indicate that RHBDF1 function is critical to the regulation of the cell growth cycle and the survival of these cancer cells.

RHBDF1 Gene Silencing Results in Autophagy in 1483 Head and Neck Squamous Cell Cancer Cells

We carried out similar studies on the effect of RHBDF1 gene silencing on 1483 head and neck cancer cells. Effectiveness of RHBDF1 gene silencing at both mRNA and protein levels was confirmed by RT-PCR and Western blotting analysis (Fig. 3A). The treatment resulted in marked inhibition of 1483 cell growth (Fig. 3B); however, unlike the breast cancer cells, which underwent apoptosis as the result, RHBDF1 gene silencing caused autophagy to the 1483 cells. To determine cell autophagy, the specific autophagy marker microtubule-associated protein 1 LC3 was conjugated with green fluorescent protein and transfected into the 1483 cells. LC3 is a mammalian homologue of the yeast Atg8 gene and is characteristically recruited to autophagic vesicles should an autophagy process takes place in the cells. The autophagic vesicles were detected as puncta accumulations of green fluorescent protein-LC3 as a result of RHBDF1 siRNA treatment (Supplementary Fig. S1).[6] Counting the number of cells that possess autophagic vesicles, we found that ~30% of the cells in RHBDF1 siRNA-treated groups were autophagic, whereas in control groups it was ~10% (Fig. 3C). To confirm this finding, we determined the lipidation of endogenous LC3-I to yield LC3-II, which marks the occurrence of an autophagy process, and found that silencing RHBDF1 in the 1483 cells gave rise to an increased amount of LC3-II in the treated cells (Fig. 3D). These results indicate that RHBDF1 gene silencing in the 1483 cells causes an significant increase of autophagy in these cells.

RHBDF1 Gene Silencing Results in a Blockage of Growth Signals

Because apoptosis and autophagy can both be caused by an inhibition of cell growth signals, we investigated the effect of RHBDF1 gene silencing on the activities of AKT and ERK, because these signaling proteins are critically involved in many signaling pathways. By using immunoprecipitation and Western blotting analysis, we found that the degree of phosphorylation of both AKT and ERK decreased in response to RHBDF1 gene silencing. The siRNA treatment caused a 60% to 70% decrease of the RHBDF1 protein level in MDA-MB-435 breast cancer cells compared with that in control siRNA-treated cells. At the same time, the extent of phosphorylation of AKT and ERK decreased by ~60% and 40%, respectively, whereas the total protein levels of these signaling proteins did not exhibit any noticeable change (Fig. 4A). Similar results were obtained with the head and neck squamous cell cancer 1483 cells, showing a decrease of the AKT and ERK phosphorylation to ~50% and 30% of control levels, respectively, when the RHBDF1 gene was silenced to give a protein level of

[6] Supplementary material for this article is available at Molecular Cancer Therapeutics Online (http://mct.aacrjournals.org/).

Published OnlineFirst June 4, 2008; DOI: 10.1158/1535-7163.MCT-08-0104

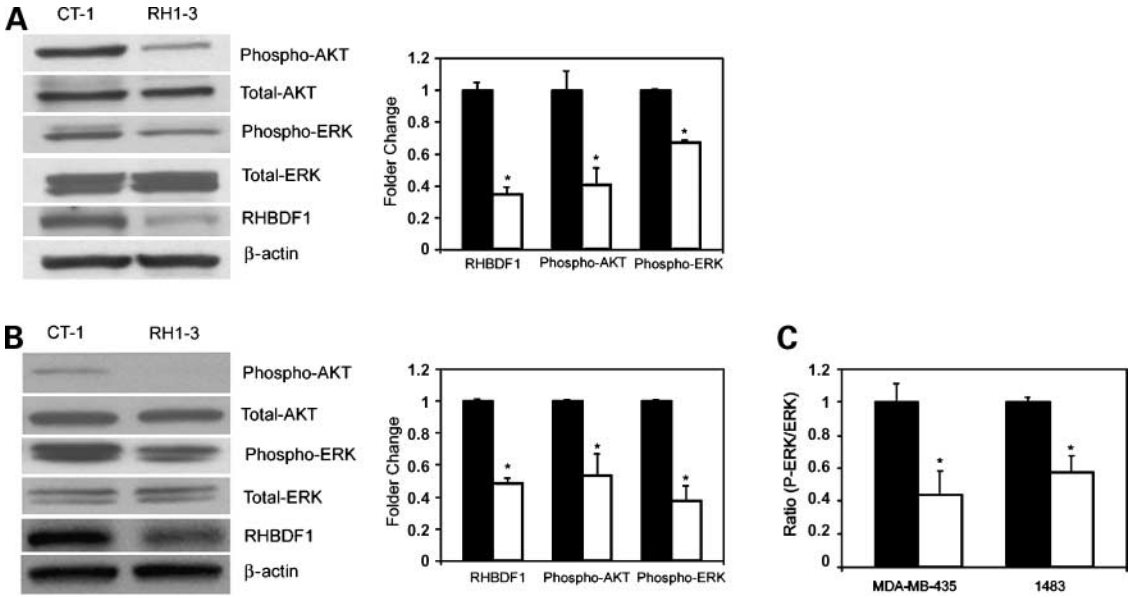

Figure 4. Down-modulation of AKT and ERK signals in RHBDF1 siRNA-treated epithelial cancer cells. **A,** quantitative analysis of Western blot analysis of AKT and ERK phosphorylation in MDA-MB-435 cells treated with either control siRNA (CT-1) or RHBDF1 siRNA (RH1-3). Relative levels of the RHBDF1, phospho-AKT, and phospho-ERK proteins in CT-1-treated cells (*black columns*) compared with those in RH1-3-treated cells (*white columns*). **B,** quantitative analysis of Western blot analysis of AKT and ERK phosphorylation levels in 1483 cells treated with either control siRNA (CT-1) or RHBDF1 siRNA (RH1-3). Relative levels of the RHBDF1, phospho-AKT, and phospho-ERK proteins in CT-1-treated cells (*black columns*) compared with those in RH1-3-treated cells (*white columns*). Values for RHBDF1, phospho-AKT, and phospho-ERK are normalized using that of β-actin, total AKT, and total ERK proteins, respectively. Mean ± SD of duplicate experiments. **C,** ELISA analysis of phospho-ERK in whole cells in MDA-MB-435 or 1483 cells treated with either control siRNA (*black columns*) or RHBDF1 siRNA (*white columns*). Mean ± SD of duplicate experiments. *, $P < 0.05$, Student's *t* test.

~50% of the control level (Fig. 4B). These findings were confirmed by using an ELISA assay that simultaneously and directly measured the level of phospho-ERK and total ERK in both MDA-MB-435 and the 1483 cells following RHBDF1 gene silencing (Fig. 4C). The ratio of phospho-ERK to total ERK decreased to ~40% in the breast cancer cells and 60% in the head and neck cancer cells. These findings indicate that both AKT and ERK activity was significantly down-modulated once RHBDF1 gene is no longer functional, suggesting that the RHBDF1 gene function is important to the maintenance of growth signal strength in these cancer cells.

Systemic Delivery of Polymer Nanoparticle-Encapsulated siRNA to Xenograft Tumors

We determined whether we were able to deliver the siRNA molecules to cancer cells in established tumors through systemic administration. We encapsulated fluorescence-conjugated siRNA molecules with the HKP nanoparticles and gave the solution to the athymic nude mice bearing 1483 xenograft tumors by tail vein injections. The average volume of the tumors at the time of treatment was ~100 mm^3. We retrieved the lung, liver, kidney, brain, and tumors at 1 min or 6 min after the injection for fluorescence microscopic analysis (Fig. 5A). We found that the siRNA molecules reached the interior of tumors within the first minute after injection, when the main body of the siRNA was found in the lung. By 60 min, a readily detectable amount of siRNA molecules was found in the tumors as well as in the liver and kidney. Little was seen in the brain possibly because of the blood-brain barrier. Further analysis revealed that the siRNA molecules were mostly deposited in proximity to the tumor vasculature (Fig. 5B). These results indicate that i.v. delivery of the HKP nanoparticle-encapsulated siRNA can gave rise to significant enrichment of the siRNA in tumor tissues.

The RHBDF1 siRNA was encapsulated with the HKP nanoparticles and given by tail vein injection (2 mg/kg) to the animals bearing 1483 xenograft (average volume, 100 mm^3). The tumors were retrieved after 48 h following the injection. We found that RHBDF1 levels were significantly lowered in the tumors of the experimental groups compared with those of the controls. Western blotting analysis showed that the amount of the RHBDF1 protein in the tumors decreased by ~50% on average ($n = 3$; $P < 0.01$, Student's *t* test; Fig. 5C). RT-PCR analysis indicated that the RHBDF1 mRNA levels decreased by about one-half on average ($n = 3$; $P < 0.01$, Student's *t* test; Fig. 5D). These results showed that we were able to silence the target gene in established xenograft tumors by using systemically delivered HKP nanoparticle-encapsulated siRNA.

HKP Nanoparticle-Encapsulated RHBDF1 siRNA Inhibits Xenograft Tumor Growth

We determined the effect of RHBDF1 gene silencing on the growth of established breast cancer MDA-MB-435 xenograft tumors. HKP-encapsulated RHBDF1 siRNA (RH1-2) was given to the tumor-bearing mice via tail vein

Published OnlineFirst June 4, 2008; DOI: 10.1158/1535-7163.MCT-08-0104

injection (2 mg/kg) on day 10 following tumor inoculation and once every 5 days thereafter for 30 days. The average volume of the tumors was ~50 mm^3 at the time of initial treatment. The RHBDF1 siRNA treatment led to a remarkable inhibition of tumor growth (Fig. 6A). Whereas both untreated (n = 6) and control siRNA-treated tumors (n = 6) exhibited typical logarithm growth rates and reached volumes ranging from 1,400 to 2,000 mm^3 during the period,

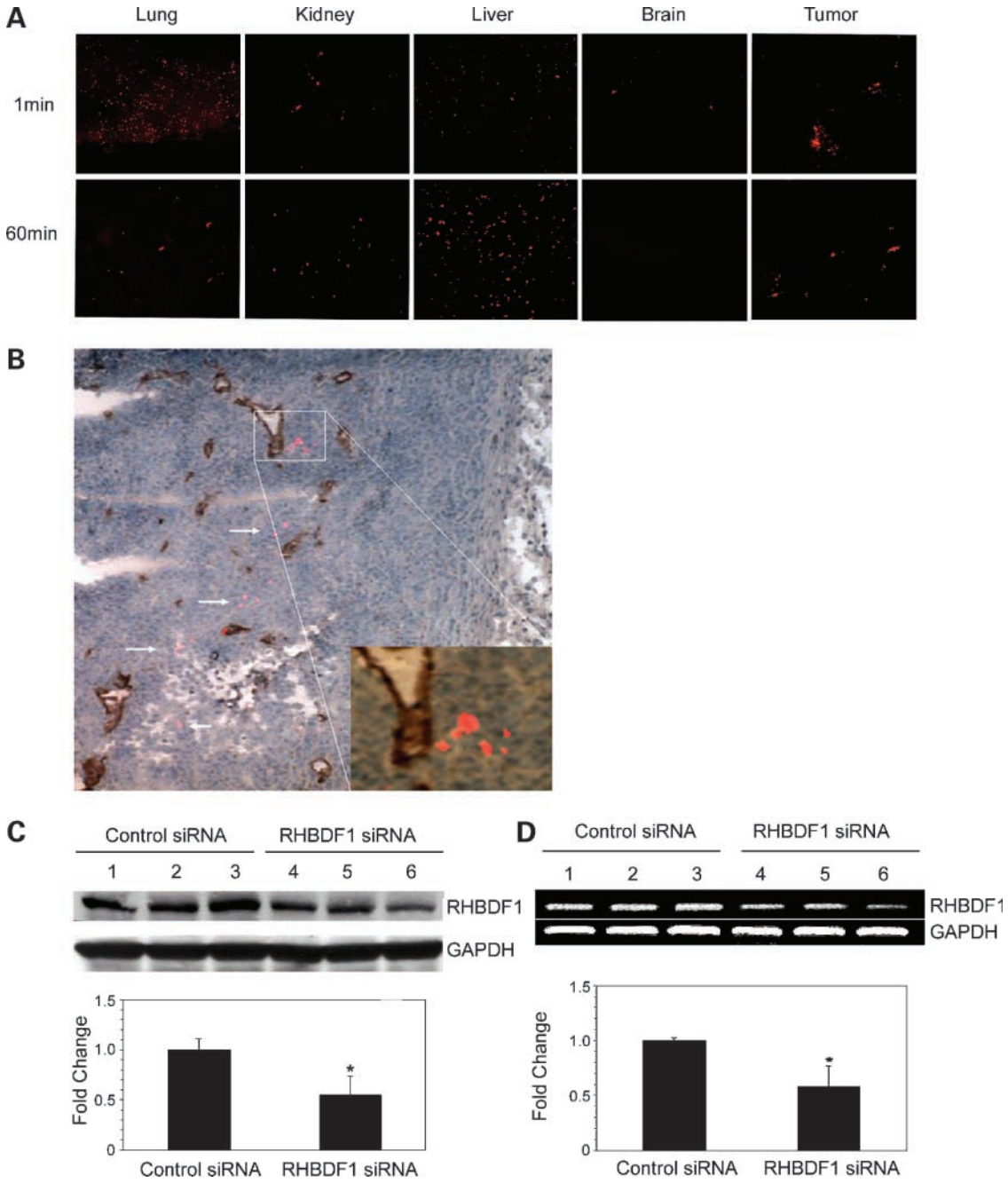

Figure 5. Accumulation of i.v. delivered HKP-encapsulated siRNA molecules in established head and neck squamous cancer 1483 xenograft tumors. **A,** images of mouse tissues and tumors with Alexa Fluor 555–labeled fluorescent siRNA CT-2 deposits following tail vein injection of HKP-siRNA. The tissues were harvested at the indicated time, freshly frozen, sectioned, and analyzed by fluorescent microscopy. Magnification, ×400. **B,** accumulation of fluorescent CT-2 (*arrows,* red deposits) in the tumors in proximity to blood vessels (*brown,* CD31 immunostaining). Magnification, ×400. *Inset,* detail showing siRNA deposits next to a blood vessel. **C,** Western blotting analysis of RHBDF1 protein levels in the xenografts of either RHBDF1 siRNA-treated animals (n = 3) or control siRNA-treated ones (n = 3). The tumors (average, 100 mm^3) were harvested after 48 h following one injection of the HKP-siRNA nanoparticles. Quantitative analysis of the Western blotting data normalized using the intensity of the glyceraldehyde-3-phosphate dehydrogenase protein. **D,** RT-PCR analysis of RHBDF1 mRNA levels in the tumors. Quantitative analysis of the RT-PCR data. Samples were the same as in **C**. *, $P < 0.05$, Student's t test.

Published OnlineFirst June 4, 2008; DOI: 10.1158/1535-7163.MCT-08-0104

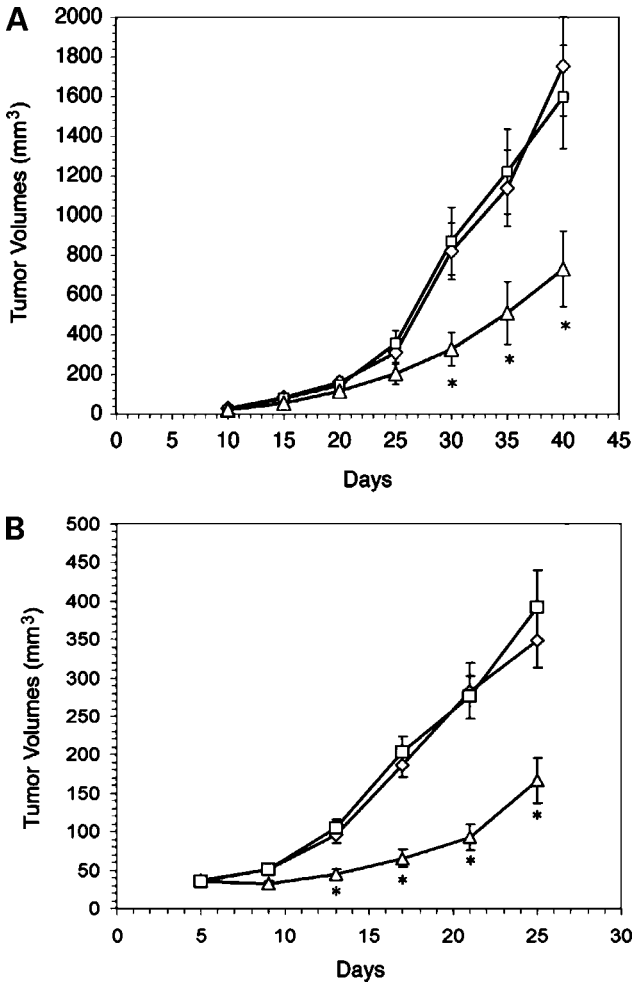

Figure 6. Inhibition of MDA-MB-435 or 1483 xenograft tumor growth by i.v. delivered HKP nanoparticle-encapsulated RHBDF1 siRNA. **A,** plots of MDA-MB-435 tumor volumes as a function of time. The tumor-bearing mice were given the HKP-siRNA solutions via tail vain injection (2 mg/kg) once every 5 d, starting on day 10 following tumor inoculation. *Diamonds,* vehicle treated ($n = 6$); *squares,* control siRNA treated ($n = 6$); *triangles,* RHBDF1 siRNA treated ($n = 6$). **B,** plots of 1483 xenograft tumor volumes as a function of time. The tumor-bearing mice were given tail vein injections of the HKP-siRNA solutions as indicated, starting on day 5 following tumor inoculation and repeated every 4 d. *Squares,* untreated ($n = 5$); *diamonds,* control siRNA treated ($n = 5$); *triangles,* RHBDF1 siRNA treated ($n = 5$). Mean ± SD. *, $P < 0.01$, ANOVA.

the RHBDF1 siRNA-treated tumors ($n = 6$) grew at a significantly reduced rate and reached an average volume of ~800 mm^3 during the same period. The experiment was repeated, and nearly identical results were obtained. These findings suggest that the RHBDF1 gene function is important to the growth of these xenograft tumors.

We repeated the experiment with a different cancer cell line, namely, the head and neck squamous cancer 1483 cells. Once the tumor volumes reached an average of 50 mm^3, we treated the tumor-bearing mice in the experimental group ($n = 5$) with HKP-encapsulated RHBDF1 siRNA RH1-2 by tail vein injection (2 mg/kg). The control groups were either untreated ($n = 5$) or treated with HKP-encapsulated control siRNA CT-1 ($n = 5$). The animals were treated once every 4 days. The tumor volumes were determined before each treatment. A substantial inhibition of the 1483 tumor growth was observed in the RHBDF1 siRNA-treated group (Fig. 6B), with the average tumor volume reaching 150 mm^3 within 25 days. No difference was observed in tumor growth rate between the CT-1 control siRNA-treated group and the untreated group, with the average tumor volumes reaching 350 and 400 mm^3, respectively, within the same period. These findings indicate that the RHBDF1 gene function is also critical to the growth of the head and neck cancer xenograft tumors.

Discussion

The RHBDF1 gene expression profile in breast cancer clinical specimens of IDC stage I of breast cancer was of great interest. It indicates a higher level of the RHBDF1 gene transcript at an early stage of breast cancer development, and possibly in breast cancer in general, suggesting that the RHBDF1 gene may have a promoting role in breast cancer progression. The RHBDF1 mRNA and protein were readily detectable in a variety of breast cancer and head and neck cancer cell lines, raising the possibility that this gene may be active in cancer cells in general.

We found that siRNA-mediated elimination of RHBDF1 in human breast cancer cell line MDA-MB-435 cells or head and neck squamous cancer cell line 1483 cells leads to marked inhibition of cell proliferation. Interestingly, however, the cause of the growth inhibition appears to be different: the MDA-MB-435 cells undergo apoptosis, whereas the 1483 cells undergo autophagy. Apoptosis and autophagy are two self-destructive processes. Apoptosis involves the activation of several catabolic enzymes, namely, caspases, in a signaling cascade, which gives rise to the rapid demolition of cellular structures and organelles, including nuclear fragmentation (12–14). Autophagy, on the other hand, represents a different process of self-destruction of cytoplasm and intracellular organelles characterized by the formation of double-membrane or multimembrane autophagic vacuoles (autophagosomes), which are eventually delivered to lysosomes for bulk degradation (15). Both autophagy and apoptosis may be triggered by common signals such as cellular stress and the inhibition of growth factor signaling (16, 17). One might thus suspect that the two processes use some common regulatory mechanisms. It has been shown, for instance, that silencing the autophagy gene ATG5 abolishes autophagy and reduces the incidence of apoptotic events in human cancer cells (18). Similarly, p53 as a potent inducer of apoptosis can also induce autophagy in a damage-regulated autophagy modulator-dependent manner or through the mammalian target of rapamycin inhibition (19, 20). It has also been shown that inhibition of the phosphatidylinositol 3-kinase/AKT pathway can activate both autophagy and apoptosis in different cells (21, 22). It is plausible that the RHBDF1 gene function is involved in a similar manner.

Published OnlineFirst June 4, 2008; DOI: 10.1158/1535-7163.MCT-08-0104

Our data show that indeed silencing the RHBDF1 gene can lead to down-modulation of key growth signals AKT and ERK. Many growth factors and mitogens use the Ras/Raf/MEK/ERK signaling cascade to transmit signals from their receptors to regulate gene expression and prevent apoptosis (23). This pathway and the Ras/phosphatidylinositol 3-kinase/PTEN/AKT pathways interact with each other to regulate cell growth (24). ERK pathway activation is of critical importance for determining specific biological outcomes, including proliferation, differentiation, and transformation. That RHBDF1 gene silencing leads to a substantial weakening of the ERK signal indicates that this novel gene is critically involved in ERK activation. In addition, the mammalian target of rapamycin pathway has been the focus of substantial interest because it integrates signals from growth factors, nutrients, or cellular energy levels (25). AKT has been shown to activate mammalian target of rapamycin (26). An alternative mechanism of mammalian target of rapamycin activation involving the ERK pathway but separate from AKT has also been elucidated recently (27, 28), involving G-protein-coupled receptor-mediated transactivation of epidermal growth factor receptor. It will therefore be very interesting to investigate the role of RHBDF1 in these signaling pathways.

Our findings indicate that RHBDF1 could be an excellent target for cancer therapy. We have shown that silencing the RHBDF1 gene in xenograft tumors can give rise to marked inhibition of tumor growth. This finding is highly significant because the same effect was seen in two xenograft tumors established by completely different cancer cell lines, namely, the breast cancer cell line MDA-MB-435 and the head and neck cancer cell line 1483. The inhibitory effect appeared sustainable as long as the animals were treated. These findings are consistent with those obtained with the cell cultures and indicate that the RHBDF1 gene has an essential function in modulating the survival and growth of the cancer cells in tumors.

A unique aspect of this study is that we successfully silenced the RHBDF1 gene in xenograft tumors by systemically administering HKP-encapsulated siRNA to the tumor-bearing mice. To our knowledge, this has rarely been achieved before. That the HKP-encapsulated fluorescent siRNA was found to accumulate in the established tumors indicates that the HKP-siRNA nanoparticles were able to home to tumors when given systemically. The mechanism of the tumor-homing effect of the HKP-siRNA nanoparticles remains to be investigated. We speculate the well-known enhanced permeability and retention effect (29), which derives from the fact that a tumor vasculature is extremely permeable (30). Another possibility is that a pH gradient from the vasculature to the cancer cells may favor the accumulation of the positively charged HKP-siRNA nanoparticles within the tumor rather than normal tissues (31).

It has recently been pointed out that the cell line MDA-MB-435 may in fact be a melanoma cell line instead of a breast cancer cell line (32, 33). However, our findings support the view that RHBDF1 remains of importance as a new target for the development of anticancer therapeutics should the cell line be reclassified. We will expand our studies in the future to include other breast cancer cell lines as well as other cancer cell lines, with the understanding that the reclassification of this cell line will affect our thinking on the molecular mechanism of the function of this thus far little known gene.

In summary, we showed that RHBDF1 function is critical to the survival of epithelial cancer cells and that RHBDF1 gene silencing can be a plausible approach to treat epithelial cancers, as the treatment may lead to inhibition of the growth of the cancer cell and causes either apoptosis or autophagy. Additionally, we showed that i.v. administration of HKP-encapsulated siRNA allows homing of the reagent to the xenografts. These findings indicate that RHBDF1 may serve as a new target for cancer therapy. Currently, we are studying whether the RHBDF1 gene function is an essential part of growth signaling pathways such as those mediated by epidermal growth factor receptor.

Disclosure of Potential Conflicts of Interest

No potential conflicts of interest were disclosed.

References

1. Koonin EV, Makarova KS, Rogozin IB, Davidovic L, Letellier MC, Pellegrini L. The rhomboids: a nearly ubiquitous family of intramembrane serine proteases that probably evolved by multiple ancient horizontal gene transfers. Genome Biol 2003;4:R19.

2. Urban S. Rhomboid proteins: conserved membrane proteases with divergent biological functions. Genes Dev 2006;20:3054 – 68.

3. Stevenson LG, Strisovsky K, Clemmer KM, Bhatt S, Freeman M, Rather PN. Rhomboid protease AarA mediates quorum-sensing in *Providencia stuartii* by activating TatA of the twin-arginine translocase. Proc Natl Acad Sci U S A 2007;104:1003 – 8.

4. McQuibban GA, Saurya S, Freeman M. Mitochondrial membrane remodelling regulated by a conserved rhomboid protease. Nature 2003;423:537 – 41.

5. Gottlieb E. OPA1 and PARL keep a lid on apoptosis. Cell 2006;126:27 – 9.

6. Dumstrei K, Nassif C, Abboud G, Aryai A, Aryai A, Hartenstein V. EGFR signaling is required for the differentiation and maintenance of neural progenitors along the dorsal midline of the *Drosophila* embryonic head. Development 1998;125:3417 – 26.

7. Nakagawa T, Guichard A, Castro CP, et al. Characterization of a human Rhomboid homolog, p100(hRho)/RHBDF1, which interacts with TGF-α family ligands. Dev Dyn 2005;233:1315 – 31.

8. Thomas SM, Bhola NE, Zhang Q, et al. Cross-talk between G protein-coupled receptor and epidermal growth factor receptor signaling pathways contributes to growth and invasion of head and neck squamous cell carcinoma. Cancer Res 2006;66:11831 – 9.

9. Kabeya Y, Mizushima N, Ueno T, et al. LC3, a mammalian homologue of yeast Apg8p, is localized in autophagosome membranes after processing. EMBO J 2000;19:5720 – 8.

10. Tanida I, Ueno T, Kominami E. LC3 conjugation system in mammalian autophagy. Int J Biochem Cell Biol 2004;36:2503 – 18.

11. Leng Q, Scaria P, Ioffe OB, Woodle M, Mixson AJ. A branched histidine/lysine peptide, H2K4b, in complex with plasmids encoding antitumor proteins inhibits tumor xenografts. J Gene Med 2006;8:1407 – 15.

12. Maiuri MC, Zalckvar E, Kimchi A, Kroemer G. Self-eating and self-killing: crosstalk between autophagy and apoptosis. Nat Rev Mol Cell Biol 2007;8:741 – 52.

13. Danial NN, Korsmeyer SJ. Cell death: critical control points. Cell 2004;116:205 – 19.

Published OnlineFirst June 4, 2008; DOI: 10.1158/1535-7163.MCT-08-0104

14. Green DR. Apoptotic pathways: ten minutes to dead. Cell 2005;121:671 – 4.

15. Mathew R, Karantza-Wadsworth V, White E. Role of autophagy in cancer. Nat Rev Cancer 2007;7:961 – 7.

16. Lum JJ, Bauer DE, Kong M, et al. Growth factor regulation of autophagy and cell survival in the absence of apoptosis. Cell 2005;120:237 – 48.

17. Takeuchi H, Kanzawa T, Kondo Y, Kondo S. Inhibition of platelet-derived growth factor signalling induces autophagy in malignant glioma cells. Br J Cancer 2004;90:1069 – 75.

18. Yousefi S, Perozzo R, Schmid I, et al. Calpain-mediated cleavage of Atg5 switches autophagy to apoptosis. Nat Cell Biol 2006;8:1124 – 32.

19. Crighton D, Wilkinson S, O'Prey J, et al. DRAM, a p53-induced modulator of autophagy, is critical for apoptosis. Cell 2006;126:121 – 34.

20. Feng Z, Zhang H, Levine AJ, Jin S. The coordinate regulation of the p53 and mTOR pathways in cells. Proc Natl Acad Sci U S A 2005;102:8204 – 9.

21. Arico S, Petiot A, Bauvy C, et al. The tumor suppressor PTEN positively regulates macroautophagy by inhibiting the phosphatidylinositol 3-kinase/protein kinase B pathway. J Biol Chem 2001;276:35243 – 6.

22. Aoki H, Takada Y, Kondo S, Sawaya R, Aggarwal BB, Kondo Y. Evidence that curcumin suppresses the growth of malignant gliomas *in vitro* and *in vivo* through induction of autophagy: role of Akt and extracellular signal-regulated kinase signaling pathways. Mol Pharmacol 2007;72:29 – 39.

23. Rozengurt E. Mitogenic signaling pathways induced by G protein-coupled receptors. J Cell Physiol 2007;213:589 – 602.

24. Wang X, Proud CG. Methods for studying signal-dependent regulation of translation factor activity. Methods Enzymol 2007;431:113 – 42.

25. Wullschleger S, Loewith R, Hall MN. TOR signaling in growth and metabolism. Cell 2006;124:471 – 84.

26. Tee AR, Anjum R, Blenis J. Inactivation of the tuberous sclerosis complex-1 and -2 gene products occurs by phosphoinositide 3-kinase/Akt-dependent and -independent phosphorylation of tuberin. J Biol Chem 2003;278:37288 – 96.

27. Roux PP, Ballif BA, Anjum R, Gygi SP, Blenis J. Tumor-promoting phorbol esters and activated Ras inactivate the tuberous sclerosis tumor suppressor complex via p90 ribosomal S6 kinase. Proc Natl Acad Sci U S A 2004;101:13489 – 94.

28. Ma L, Chen Z, Erdjument-Bromage H, Tempst P, Pandolfi PP. Phosphorylation and functional inactivation of TSC2 by Erk implications for tuberous sclerosis and cancer pathogenesis. Cell 2005;121:179 – 93.

29. Baban DF, Seymour LW. Control of tumour vascular permeability. Adv Drug Deliv Rev 1998;34:109 – 19.

30. Dvorak HF. Tumors: wounds that do not heal. Similarities between tumor stroma generation and wound healing. N Engl J Med 1986;315:1650 – 9.

31. Ashby BS. pH studies in human malignant tumours. Lancet 1966;2:312 – 5.

32. Rae JM, Creighton CJ, Meck JM, Haddad BR, Johnson MD. MDA-MB-435 cells are derived from M14 melanoma cells—a loss for breast cancer, but a boon for melanoma research. Breast Cancer Res Treat 2007;104:13 – 9.

33. Christgen M, Lehmann U. MDA-MB-435: the questionable use of a melanoma cell line as a model for human breast cancer is ongoing. Cancer Biol Ther 2007;6:1355 – 7.

AACR American Association for Cancer Research

Molecular Cancer Therapeutics

Human rhomboid family-1 gene silencing causes apoptosis or autophagy to epithelial cancer cells and inhibits xenograft tumor growth

Zhenwen Yan, Huafei Zou, Fang Tian, et al.

Mol Cancer Ther 2008;7:1355-1364. Published OnlineFirst June 4, 2008.